RESEARCH ARTICLE

Fault Tolerance Method of Low-Resolution Hall Sensor in Permanent Magnet Synchronous Machine

CHUANGQIANG GUO[1,2], **(Member, IEEE), XINDONG GAO**[1], **QINGLI ZHANG**[3], **AND YINGYUAN ZHU**[1]

[1]Harbin Institute of Technology, Harbin 150000, China
[2]HIT Wuhu Robot Technology Research Institute, Wuhu 241000, China
[3]China Academy of Launch Vehicle Technology, Beijing 100076, China

Corresponding author: Yingyuan Zhu (dirzhuyy@aliyun.com)

ABSTRACT The estimation of the motor rotor positions with high-precision based on low-resolution Hall sensors becomes an important trend to realize the vector control in low-cost permanent magnet synchronous machine (PMSM) based control systems. Most existing studies focus on the methods to improve the estimating precision of rotor positions, while the estimating precision of failed Hall sensors and the corresponding control strategies for fault tolerance is rarely explored. This paper proposes a method that can online estimate the position of a PMSM rotor with fault detection and fault tolerance. Such a method can achieve both stable and precise estimations on rotor position even when one or two Hall sensors fail. Meanwhile, it can meet the needs of vector control under variable speed and load on the PMSM. Finally, a dSPACE-based semi-physical simulation platform is established, which is used to validate the effectiveness of the proposed method with multiple experiments.

INDEX TERMS Permanent magnet synchronous machine, hall sensor, fault detection, fault tolerance.

I. INTRODUCTION

In view of the multiple advantages of permanent magnet synchronous machines (PMSMs) such as high energy density, high operation efficiency, and easy controller design, it has been widely applied to domestic, industrial, and military fields, including robotics, electric vehicles, electric aircraft and submarines [1], etc. Among the control technologies of PMSM, field-oriented control (FOC) has become the most widely used control strategy of PMSM because it can decouple the motor flux and output torque [2]. To realize FOC, an accurate rotor position of PMSM is necessary for the coordinate transformation of phase current from the three-phase static coordinate system (a-b-c), two-phase static coordinate system (α-β), to another two-phase rotating coordinate

The associate editor coordinating the review of this manuscript and approving it for publication was Yu Wang.

system (d-q). Such information on the rotor position commonly requires the availability of encoders or resolver on the motor axis. Nevertheless, this design increases the length of the motor axis and the volume and cost of the device. Therefore, most studies attempt to research the position estimation methods of PMSM rotors without position sensors or based on low-resolution Hall sensors, to fulfill the low-cost requirements of PMSM control system design.

The position estimation methods for PMSM rotors without position sensors are realized by the combination of the inspected voltage and current information of motor winding and the approximated PMSM models, including the direct calculation method, inductance change-based observer algorithm, model reference adaptive method [3], etc. However, these methods can only work in the PMSMs with medium or high rotational speed. When a PMSM rotor rotates at a low speed, the back electromotive force and the current

value of the PMSM are minimal, and the PMSM suffers from noise interference, requiring high- or low-frequency signal injection or even other position estimation methods to alleviate these drawbacks [4]. Such method can achieve satisfactory results in a suitable range of rotational speeds. However, there is no appropriate method that can estimate the positions of PMSM rotors in a full range of rotational speed without the use of position sensors [5]. Therefore, the control method of PMSM without position sensors is not suitable for applications with a wide speed regulation range.

The position estimation methods for PMSM rotors based on low-resolution position sensors can be achieved by the use of low-resolution position information from switch-type Hall sensors to estimate the PMSM rotor position for constructing the closed-loop control. K. A. Corzine et al. proposed to use the concept of average rotational speed to estimate the rotor position of a PMSM [6]. S. Morimoto et al. and J. Bu et al. introduced PMSM acceleration parameters in the position estimation method to increase the estimating precision during the rotational speed changes of the PMSM [7], [8]. A. Yoo et al. utilized two serial observers to estimate the position of a PMSM rotor [9]. Although such a method can increase the estimating prevision, the observer parameters are related to the dynamic characteristics of the PMSM during operation. S. Y. Kim et al. proposed a full-order Romberg position observer established by a mathematical model of a PMSM and the related motion equations, which has a small delay in position estimation, high accuracy, and good dynamic characteristics [10].

Most of the research on the position estimation methods consider that all of the three Hall position sensors can perform the function properly. However, any or all of the three sensors may fail to work due to various reasons, such as extreme change of operational environment, vibration, shorted or open connection, etc. Failure of Hall sensors can lead to speed fluctuations, reduced position accuracy, and reduced safety of mechanical systems. To improve the reliability of the position estimation method, detailed research on the fault tolerance position estimation method from failed Hall position sensors seems to be very desirable [11]. Mousmi et al. proposed a fault tolerant control (FTC) method based on sensorless controls [12]. However, Jeong et al. believed that Mousmi's method needs a series of accurate machine parameters, which requires higher computational power [13]. In literature [14], a fault diagnosis (FD) algorithm was developed to identify the Hall position sensor faults based on Discrete Fourier Transform (DFT) analysis of the measured line-to-line voltages, which will also increase the consumption of computational resources greatly. Zhang and Feng proposed a fast fault diagnosis (FFD) method for analyzing different fault cases and diagnosing faulty signal(s) [15]. However, the method has not been used in the FOC of PMSM directly. In summary, most of the research on the position estimation methods based on Hall position sensors attempt to improve the precision of position calculation, while the research on the fault tolerance position estimation method from failed Hall sensors is less [16].
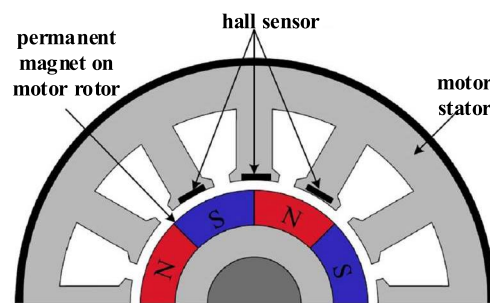

FIGURE 1. Installation of hall sensor and working principle [17].

This paper aims to the needs of the position estimation of PMSM rotors from Hall position sensors and proposes a method that can realize online fault detection and fault tolerance based on a hybrid position observer. Finally, a large number of experiments verify the effectiveness of the proposed method.

II. ROTOR POSITION ESTIMATION METHOD BASED ON HYBRID OBSERVER
A. HALL SIGNAL
Fig. 1 illustrates the installation of a Hall position sensor on a PMSM and its working principle, where three Hall sensors are spaced at an electrical angle of $2\pi/3$ apart from each other. For convenience, all rotor angles hereinafter refer to electrical angles. When the Hall sensor detects that the magnetic field strength of the rotor magnet steel is higher than the chip design threshold (i.e., the permanent magnet N pole is close to the Hall element), it outputs a high-level signal, while the Hall sensor detects that the reverse magnetic field strength is higher than the chip design threshold (i.e., the S pole of the permanent magnet is close to the Hall element), it outputs a low-level signal. Since the N poles and S poles of the permanent magnets on the rotor are alternately arranged at equal intervals, all of the three Hall position sensors can output square wave signals (H_a, H_b, and H_c) with a period of π, and the phase differences of the three signals are all $2\pi/3$. Under normal conditions, according to the combination of the output signals from the three Hall sensors H_s ($H_s = 4H_a + 2H_b + H_c$), there are six valid non-zero states, where each state corresponds to an interval of $\pi/3$, as shown in Fig. 2. When the motor rotates clockwise, the normal H_s changes in the order of $3\rightarrow1\rightarrow5\rightarrow4\rightarrow6\rightarrow2\rightarrow3$; when the motor rotates counterclockwise, the normal H_s changes in the order of $3\rightarrow2\rightarrow6\rightarrow4\rightarrow5\rightarrow1\rightarrow3$. However, there will be many types of faults occurring in hall position sensors due to various reasons. For example, (a) the controller will get a constantly high or low status when the signal line short-circuits with the power supply or ground, (b) the hall position sensors will generate several interfering pulse signals with short duration when the power supply voltage fluctuates or subjects to a strong magnetic or electric field interference, (c) the hall position sensors will trigger an error state when an abnormal gap appears on the rotor magnet, etc. However,
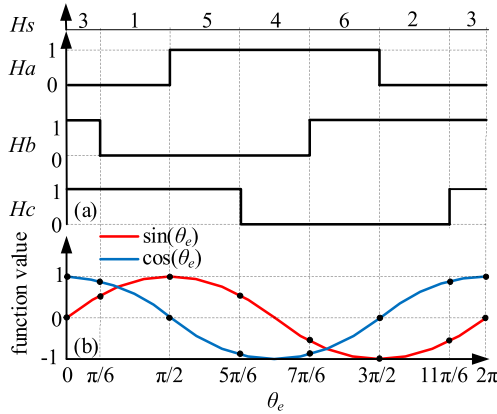
FIGURE 2. Relationship between states of Hall Sensor and sine and cosine of PMSM rotor angle.
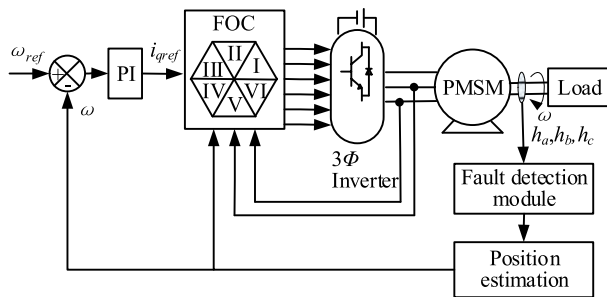

FIGURE 3. Block diagram of fault-tolerant vector control in PMSM driving system.

FIGURE 4. Rotor position estimation method based on hybrid position observer.

the fault mode (a) the controller gets a constantly high or low value (or values) seems to be the exclusive mode studied most widely. For example, only fault mode (a) was considered in the literature [14], [15]. Therefore, only fault mode (a) will be discussed in this paper.

Fig. 3 gives the block diagram of the adopted PMSM driver system, which consists of a DC power, a voltage source inverter, a PMSM with a three-phase star configuration, and a workload. Three current sensors are employed to measure the current in each phase of the stator. Three hall position sensors are installed on the shaft of the motor, perceiving the information of speed and position for the speed controller. The fault detection module is used to realize the online fault detection of Hall position sensors. The position estimation module is used to realize high-precision position estimation of the PMSM rotor according to the position information from the failed Hall sensor. FOC control, which relies on the space vector pulse width modulation (SVPWM) strategy, is used to provide three-phase balanced sinusoidal currents to the PMSM.

B. POSITION ESTIMATION METHOD

The proposed position estimation method is based on a hybrid position observer, which utilizes the input H_s to estimate the current position of the PMSM rotor θ_e. Fig. 2 also provides the relationship between the states of the Hall sensor and the $\sin(\theta_e)$ and $\cos(\theta_e)$ of θ_e. It can be seen that in the same
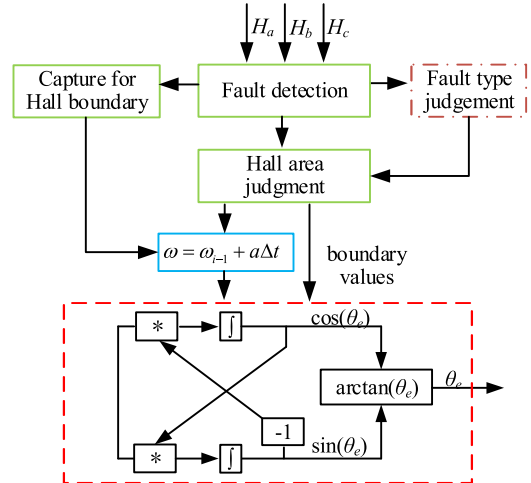
electrical angle cycle of the PMSM rotor, when the state of any one of the three Hall sensors changes, a set of accurate sine and cosine values corresponding to the position of the PMSM rotor can be obtained, where these two values can be calculated by

$$\frac{d\sin(\theta_e)}{dt} = \omega_e \cos(\theta_e) \quad (1)$$

and

$$\frac{d\cos(\theta_e)}{dt} = -\omega_e \sin(\theta_e) \quad (2)$$

where ω_e refers to the angular velocity of the PMSM rotor. The value of ω_e is got by the difference calculating of discrete position information from Hall sensors of PMSM. When the three Hall sensors of the PMSM are all normal, the discrete position information provided by the three Hall sensors will participate in the calculation. However, when one or two Hall sensors fail, only the position information provided by the remaining normal Hall sensors will participate in the calculation. In addition, in order to reduce the impact of speed changes on the position estimation accuracy, the expected acceleration is used as a feedforward signal for speed estimation.

By Integrating both sides of the Eqs. (1) and (2), we can get

$$\sin(\theta_e) = \omega_e \int_{\theta_{\min}}^{\theta_{\max}} \cos(\theta_e)dt + \sin(\theta_{\min}) \quad (3)$$

and

$$\cos(\theta_e) = -\omega_e \int_{\theta_{\min}}^{\theta_{\max}} \sin(\theta_e)dt + \cos(\theta_{\min}) \quad (4)$$

where θ_{max} and θ_{min} refer to the maximum and minimum angle values of the current Hall angle sector where the rotor is located.

TABLE 1. Hall boundary constants of hybrid observer.

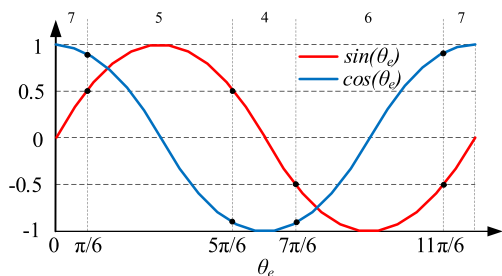| H_s	Hall boundary constants					
	max(sin(θ_{ei}))	min(sin(θ_{ei}))	max(cos(θ_{ei}))	min(cos(θ_{ei}))	sin(θ_{mini})	cos(θ_{mini})
3	sin(π/6)	sin(11π/6)	cos(0)	cos(π/6)	sin(11π/6)	cos(11π/6)
1	sin(π/2)	sin(π/6)	cos(π/6)	cos(π/2)	sin(π/6)	cos(π/6)
5	sin(π/6)	sin(5π/6)	cos(π/2)	cos(5π/6)	sin(π/2)	cos(π/2)
4	sin(5π/6)	sin(7π/6)	cos(π)	cos(5π/6)	sin(5π/6)	cos(5π/6)
6	sin(5π/6)	sin(3π/2)	cos(3π/2)	cos(7π/6)	sin(7π/6)	cos(7π/6)
2	sin(11π/6)	sin(3π/2)	cos(11π/6)	cos(3π/2)	sin(3π/2)	cos(3π/2)

FIGURE 5. Values of failed Hall boundary constant at $H_a \equiv 1$.

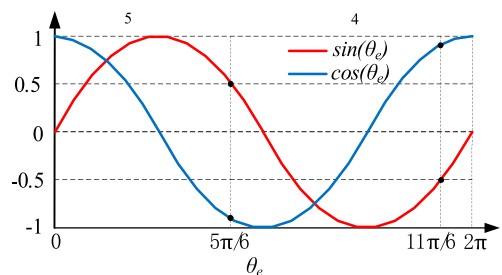**FIGURE 6.** Values of Hall boundary constant at Ha ≡ 1 and Hb ≡ 0.

After obtaining $\sin(\theta_e)$ and $\cos(\theta_e)$, the current rotor angle θ_e can be calculated by the arctangent function:

$$\theta_e = \arctan(\sin(\theta_e)/\cos(\theta_e)) \qquad (5)$$

Fig. 4 gives the block diagram of the PMSM rotor position estimation method with fault tolerance, including a fault detection module for Hall sensors, a fault type judgment module for Hall sensors, a Hall area judgment module for the PMSM rotor, a capture module for Hall boundary states, etc. When calculating the sine and cosines, the boundary values (i.e., max($\sin(\theta_e)$), min($\sin(\theta_e)$), max($\cos(\theta_e)$), and min($\cos(\theta_e)$)) and the initial value of the integral (i.e., $\sin(\theta_{min})$ and $\cos(\theta_{min})$) and other six hybrid observer boundary constants. When there are no failed Hall sensors, the boundary constants of each Hall sector are shown as the black dots in Fig. 2. The values of the Hall boundary constant of the hybrid observer are shown in Table 1, where max($\sin(\theta_{ei})$), min($\sin(\theta_{ei})$), max($\cos(\theta_{ei})$), and min($\cos(\theta_{ei})$) represent the upper and lower values of the sine and the cosine integral

in the i-th Hall electrical angle interval, and $\sin(\theta_{mini})$ and $\cos(\theta_{mini})$ represent the initial values of the sine and cosine integral.

When any one of the Hall sensors fails, the size and number of the Hall electrical angular intervals change due to the lack of part of the Hall signal. It is necessary to change the input constant of the corresponding electrical angle interval according to the fault type of the Hall sensor for achieving the fault-tolerant control of the hybrid position observer. Figs. 5 and 6 show the Hall boundary values under the conditions of one failed Hall sensor ($H_a \equiv 1$, $H_b \equiv 0$) and two failed Hall sensors ($H_a \equiv 1$, $H_b \equiv 0$), respectively. When there is one Hall sensor fails, the update frequency of the Hall boundary constant is reduced from six times in one electrical angle cycle to four times; when both Hall sensors fail, the update frequency of the Hall boundary constant becomes twice a cycle.

III. HALL SIGNAL DETECTION METHOD

The prerequisite for realizing fault-tolerant control is to online identify the fault location of the fault in real-time. A Hall signal acquisition circuit system is usually composed of a Hall sensor chip, a power supply circuit, a filter circuit, etc. The state of the output logic signal is either 0 or 1, where the failure reason includes power failure, short circuit between the output signal and power supply (or ground), open circuit of the output signal, etc. [18]. When the fault occurs, the controller obtains either 0 or 1 for the Hall states (the same as fault state), which will remain no matter how the PMSM rotor angle changes. There are a total of 20 different fault types according to the different fault state combinations of the three Hall sensors. Note that when all three hall sensors fail, the control method without position sensor is not within the scope of this work, only 18 fault types of hall sensors (ie 1 or 2 fault hall sensors) are discussed, where the fault type is denoted as f. As shown in the third column of Table 2, each fault type has a different sequence of Hall states. When there are one or two Hall sensors fail and the values are identical after the failure, the Hall signal state will be either 7 or 0 (both 7 and 0 do not appear in the normal state); when both Hall sensors fail and the values are not identical, the two Hall states alternately change and are not equal to either 7 or 0.

To realize fault detection, a detection variable m is designed, as formulated in Eq. 6, where H_{sn}, H_{sn-1}, and H_{sn-2} are three adjacent Hall states. Since the principle of fault detection during the clockwise and counterclockwise movement of the PMSM is the same, the following contents will take clockwise movement as an example for illustrating the fault detection method. When the hall signal works normally, it changes in the order of 3→1→5→4→6→2→3, and the value of the detection variable m is either 0 or 7; when one or two hall sensors fail and the values are identical, H_{sn} will be equal to either 0 or 7. In order to ensure the uniqueness of the value of m, the state where H_{sn} is identical to either 0 or 7 is the initial state of the detection sequence. When both two Hall sensors fail and the value are not identical, each fault type

TABLE 2. Scalar feature sequence after Hall sensor fail.

Fault	Fault Type f	Fault State	Ssequence of Hall States	Detection Ssequence	Detection Variable m
One Hall sensor fails	1	$H_a \equiv 1$	7→5→4→6→7	7→5→4	6
	2	$H_a \equiv 0$	0→2→3→1→0	0→2→3	1
	3	$H_b \equiv 1$	7→6→2→3→7	7→6→2	3
	4	$H_b \equiv 0$	0→1→5→4→0	0→1→5	4
	5	$H_c \equiv 1$	7→3→1→5→7	7→3→1	5
	6	$H_c \equiv 0$	0→4→6→2→0	0→4→6	2
Two Hall sensors fail	7	$H_a \equiv 0,$ $H_b \equiv 0$	0→1→0→1	0→1→0	-1
	8	$H_a \equiv 0,$ $H_b \equiv 1$	*3→2→3→2*	*3→2→3* or *2→3→2*	*4 or 1*
	9	$H_a \equiv 1,$ $H_b \equiv 0$	*5→4→5→4*	*5→4→5* or *4→5→4*	*6 or 3*
	10	$H_a \equiv 1,$ $H_b \equiv 1$	7→6→7→6	7→6→7	8
	11	$H_a \equiv 0,$ $H_c \equiv 0$	0→2→0→2	0→2→0	-2
	12	$H_a \equiv 0,$ $H_c \equiv 1$	*3→1→3→1*	*3→1→3* or *1→3→1*	*5 or -1*
	13	$H_a \equiv 1,$ $H_c \equiv 0$	*6→4→6→4*	*6→4→6* or *4→6→4*	*8 or 2*
	14	$H_a \equiv 1,$ $H_c \equiv 1$	7→5→7→5	7→5→7	9
	15	$H_b \equiv 0,$ $H_c \equiv 0$	0→4→0→4	0→4→0	-4
	16	$H_b \equiv 0,$ $H_c \equiv 1$	*1→5→1→5*	*1→5→1* or *5→1→5*	*-3 or 9*
	17	$H_b \equiv 1,$ $H_c \equiv 0$	*2→6→2→6*	*2→6→2* or *6→2→6*	*-2 or 10*
	18	$H_b \equiv 1,$ $H_c \equiv 1$	7→3→7→3	7→3→7	11

FIGURE 7. Experimental setup.

has two fault detection sequences, correspond to two different values of m, where the two detection variables correspond to different fault states, as highlighted in bold and italic font in Table 2. Therefore, the failed sensor can be identified by the digital Hall state and the detection variable m, and then the fault type f can also be obtained according to m.

$$m = H_{sn} + H_{sn-2} - H_{sn-1}. \qquad (6)$$

Above all, the proposed method can realize fault detection by judging the sequence of three-phase Hall sensors. Based on the detected fault type of the Hall sensor, the method further realizes the fault-tolerant control of Hall sensors by changing the boundary condition of normal position estimation method. Compared with the traditional FTC methods proposed in the literature [3], [5], and [12], the presented method only needs to add little logical judgment and assignment operation, so it is very suitable for the low-cost PMSM control system with limited computing power, due to the advantage of the small amount of calculation.

IV. EXPERIMENTAL RESULTS AND DISCUSSIONS
A. SETUP
Fig. 7 provides a system for the experiments on testing and validating the proposed fault detection and fault tolerance
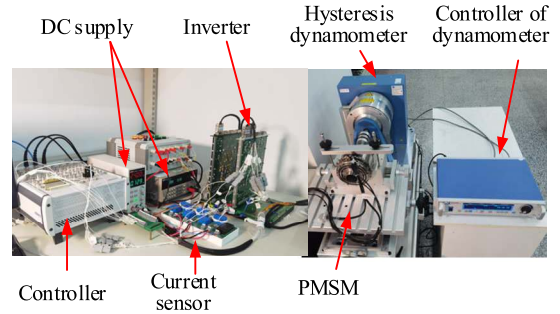
methods. This system is composed of a MicroLab controller as the core of semi-physical simulation platform, which generates a pulse width modulation signal with a carrier frequency of 10KHz for the voltage source inverter. The voltage source inverter uses the three-phase full-bridge motor driver chip IR2130D and the MOSFET chip IRFP240 produced by International Rectifiers as the core electronic components, where the dead time of IR2130D is 2 μs. During the experiment, a surface-mounted PMSM is used, the rotor is designed with eight pairs of magnetic poles, the motor torque coefficient is 4.26 Nm/A, and the rated current is 2A. The PMSM is designed with three digital Hall position sensors and a resolver. The state of the Hall sensor changes 48 times in one rotation cycle of the PMSM rotor, while the resolver data changes 2^{18} times. The resolver information does not participate in closed-loop control and is only used for evaluating the precision of the estimated position of the PMSM rotor by the Hall position sensors. The PMSM rotor is connected to the hysteresis dynamometer, and the torque applied to the rotor can be accurately adjusted through the built-in controller of the hysteresis dynamometer. During the experiment, the DC voltage of the motor drive inverter is set as 100V, and the fault states of the Hall sensors are simulated by modifying the actual output value of the sensor through software.

B. SETUP PERFORMANCE OF POSITION ESTIMATION
In order to verify the effect of PMSM vector control based on the rotor position estimated by the Hall position sensors, speed step and load shock experiments are carried out. During the experiment, the motor runs stably with an initial load of zero Nm and an expected speed of 150 r/min. Then, a load of 0.5 Nm is applied at about 4.0 s. At about 12.5 s, the desired speed is increased to 250 r/min. Fig. 8(a) shows the speed curve during the experiment. It can be seen that when a load of 0.5 Nm is applied to the motor, the motor speed decreases and back to the target speed after about 1.5 s; when the expected speed changes stepwise, the actual speed of the motor has a slight overshoot and reaches the target value quickly, and then remains stable run. From Fig. 8(b), it can be seen that the three-phase current of the motor can respond promptly to the changes in load and the expected speed while ensuring that the three-phase sinusoidal current has symmetrical
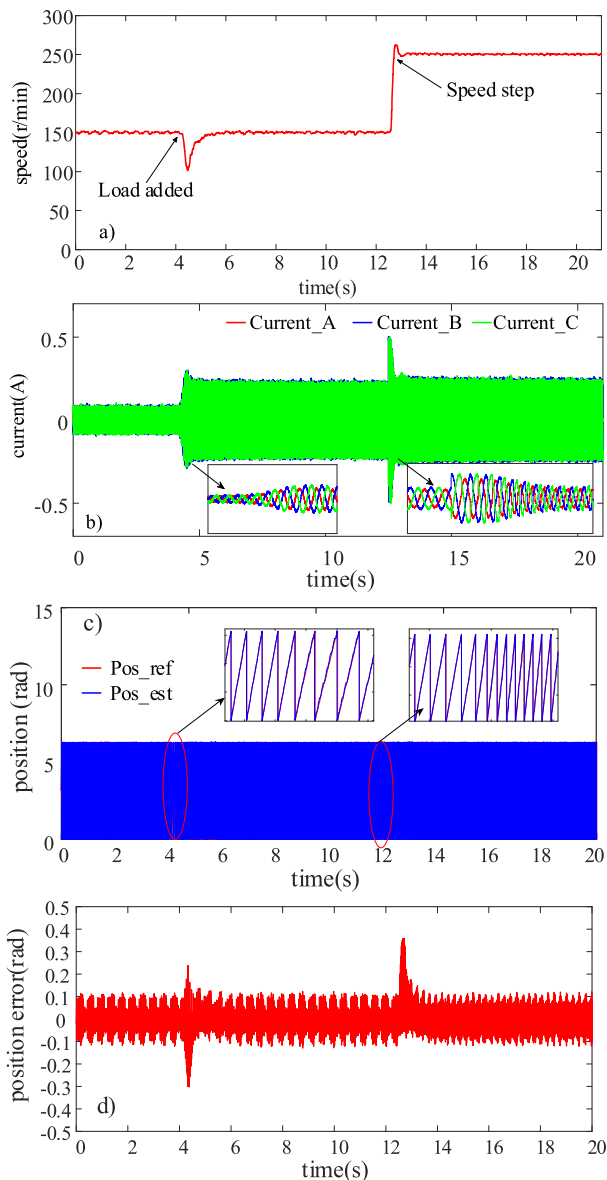
FIGURE 8. Experimental results on characteristics of Hybrid position observer with dynamic loads. (a) Motor speed. (b) Three-phase current. (c) Estimated rotor position and the reference position. (d) Error of position estimation.

waveforms, smooth curves, and stable amplitudes. Take the position information of the resolver installed on the motor shaft as a reference, Fig. 8(c) provides the estimated rotor position(Pos_est) and the reference position (Pos_ref) in the experiment. Fig. 8(d) provides the deviation between the estimated rotor position and the reference position in the experiment, where the maximum estimated error is 0.35 rad, which meets the needs of normal motor motion.

C. EXPERIMENTS ON FAULT DETECTION AND FAULT TOLERANCE

Fig. 9 gives the results of the fault detection based on the sequence of Hall states, where the operating speed of the PMSM is 200 r/min and the load is 0.2 Nm. The failure

of the Hall position sensor is simulated by software, which sets the A-phase of the Hall state to '1' at time =∼4s to simulate the failure of a single Hall sensor and set the B-phase of the Hall state to '0' at time =∼9s (under the failure of the A-phase of the first Hall sensor) for simulating the failure of both Hall sensors. Fig. 9(a) provides the detection results of the Hall sensors. About 30ms after the Hall states of phases A and B, the software recognizes the fault states '1' and '9', respectively, which are consistent with the fault types listed in Table 2. Fig. 9(b) shows the three-phase current waveforms of the PMSM before and after the failure of the Hall sensors. The motor phase current amplitude is about 0.2A before the failure occurs; when the A-phase Hall sensor fails, the motor phase current amplitude increases to 0.3A and then returns to the normal value of 0.2A after about 0.1s. When the B-phase Hall sensor fails at the same time, the motor phase current amplitude increases to 0.5A and then returns to the normal value of 0.2A after about 0.5s. Fig. 9(c) describes the motor speed curve during the fault-tolerant experiment. After the failure of the A-phase Hall sensor, the speed output fluctuates slightly, where the duration is about 0.5s and the maximum speed change is about 10 r/min; when the B-phase Hall sensor fails, the speed fluctuation amplitude increases, where the duration is about 1s and the maximum speed change is about 30 r/min. Fig. 9(d) and Fig.(e) give the estimated position and the position estimation error of the PMSM rotor respectively. When the A-phase Hall sensor fails, the maximum position estimation error is about 1 rad; when the B-phase Hall sensor fails at the same time, the maximum position estimation error is about 4.5 rad. Through the above experimental results, it can be found that the developed fault detection method can efficiently identify the failed Hall sensors. Besides, the fault-tolerant control algorithm can effectively isolate the failed Hall sensors and provide accurate information on the rotor position. Furthermore, both the motor speed and the fluctuation amplitude of its phase current are small, which can be controlled to return to the normal value in time.

D. EXPERIMENTS ON DYNAMIC CHARACTERISTIC OF PMSM WITH FAULT-TOLERANCE

In order to validate that the hybrid position observers based PMSM fault-tolerant vector control can cope with the failure of Hall sensors, the dynamic characteristics of the PMSM after the failure of the two Hall sensors are tested, where the results are shown in Fig. 10. During the experiment, the initial target speed of the motor is 150 r/min. Fig. 10(a) gives the changes in the three-phase current of the PMSM. At time index 1, the load torque increases from 0 Nm to 0.2 Nm; at time index 2, the load torque gradually increases to 4 Nm; at time index 3, the target speed of the PMSM has a step change from 150 r/min to 230 r/min. It can be seen from Fig. 10(a) that the three-phase current waveforms of the PMSM are symmetrical and stable without significant distortion. Besides, the motor speed curve shown in Fig. 10(b) shows that the speed drops suddenly when a load is applied and then returns to the normal value in about 0.8s,
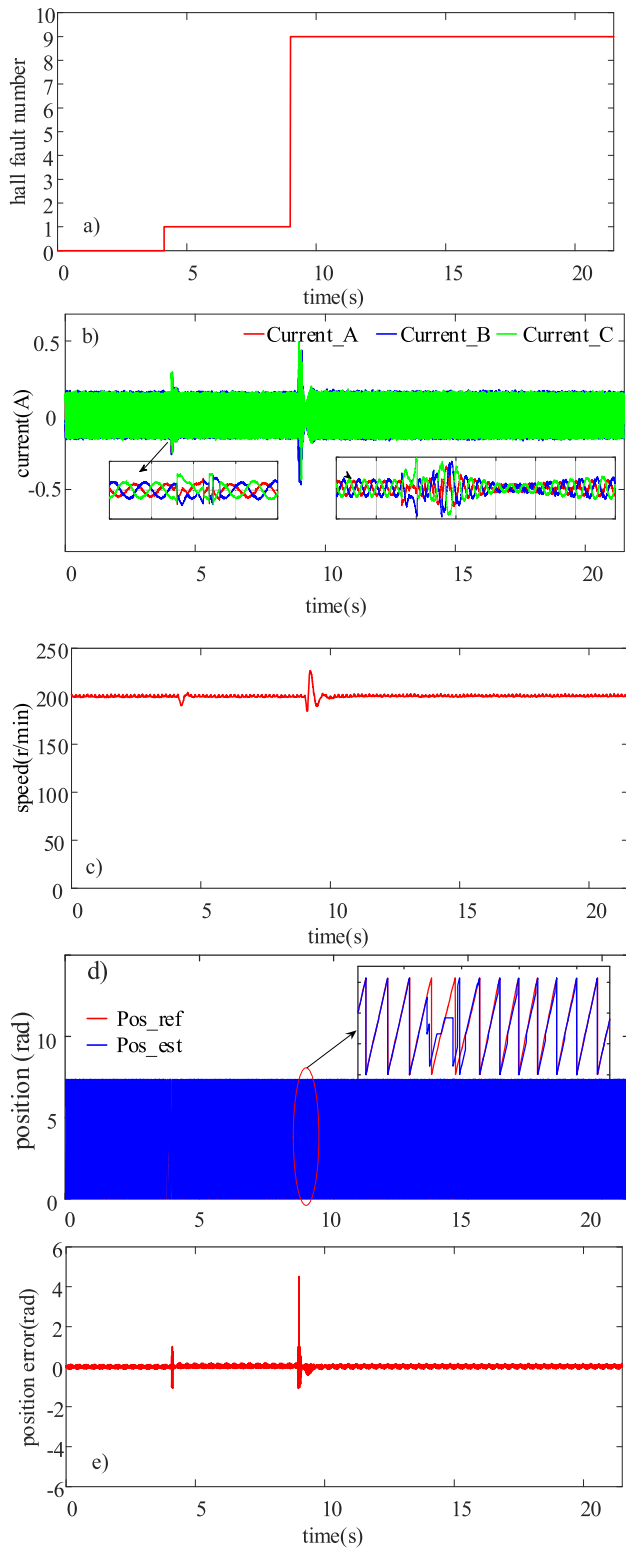
FIGURE 9. Experimental results on fault-tolerance of hybrid Hall sensors. (a) Fault detection. (b) Three-phase current. (c) Motor speed. (d) Estimated rotor position and the reference position. (e) Error of position estimation.

FIGURE 10. Experimental results on dynamic characteristics of hybrid position observers based fault-tolerant control. (a) Three-phase current. (b) Motor speed. (c) Estimated rotor position and the reference position. (d) Error of position estimation.

PMSM rotor respectively. The maximum position estimation error is about 0.9 rad. When the A-phase Hall sensor fails, the maximum position estimation error is about 1 rad; Therefore, the developed fault-tolerant control method based on the hybrid position observers has a certain anti-interference ability when two Hall sensors fail, which meets the basic requirements for operation.

V. CONCLUSION

In order to improve the reliability of the PMSM estimation algorithm based on low-resolution Hall position sensors, this paper proposes an online fault detection and fault-tolerant position estimation method for a PMSM that can achieve high-precision position estimation with failed Hall position

demonstrating that the motor can effectively track the expected speed and operate stably. Fig. 10(c) and Fig.(d) give the estimated position and the position estimation error of the
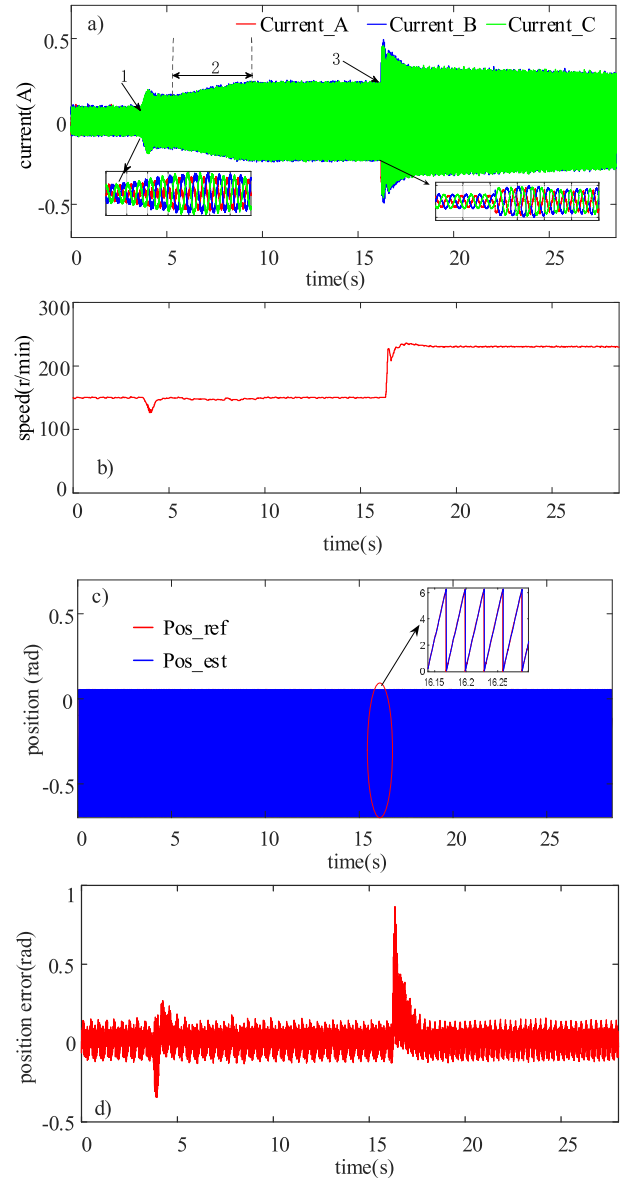
sensors. This method is designed to work with different sequences of Hall states under different fault types, based on the encoding of scalar Hall states, which realizes online detection and positioning under one or two failed Hall sensors. Through the improvement of a hybrid position observer-based position estimation method for the PMSM rotor, the proposed method is endowed with the capability of fault tolerance by utilizing the fault information of Hall sensors for the online adjustment of the boundary conditions of the observers. Such a mechanism ensures the availability of the rotor position information under one or two failed Hall sensors. Finally, a dSPACE-based platform is established to validate the reliability and robustness of the proposed fault-tolerant method. Since the proposed method only needs to add little logic judgment and assignment operation, compared with the existing FTC methods, it is very suitable for the low-cost PMSM control system with limited computing power.

REFERENCES

[1] W. Wang, M. Cheng, B. Zhang, Y. Zhu, and S. Ding, "A fault-tolerant permanent-magnet traction module for subway applications," *IEEE Trans. Power Electron.*, vol. 29, no. 4, pp. 1646–1658, Apr. 2014.

[2] C. Chakraborty and V. Verma, "Speed and current sensor fault detection and isolation technique for induction motor drive using axes transformation," *IEEE Trans. Ind. Electron.*, vol. 62, no. 3, pp. 1943–1954, Mar. 2015.

[3] C. Hoe Ng, M. Rashed, P. Vas, F. Stronach, and P. MacConnell, "A novel MRAS current-based sensorless vector controlled PMLSM drive for low speed operation," in *Proc. IEEE Int. Electr. Mach. Drives Conf. (IEMDC)*, Jun. 2003, pp. 1889–1894. [Online]. Available: https://ieeexplore.ieee.org/document/1210710

[4] M. J. Corley and R. D. Lorenz, "Rotor position and velocity estimation for a salient-pole permanent magnet synchronous machine at standstill and high speeds," *IEEE Trans. Ind. Appl.*, vol. 34, no. 4, pp. 784–789, Jul. 1998.

[5] T.-W. Chun, Q.-V. Tran, H.-H. Lee, and H.-G. Kim, "Sensorless control of BLDC motor drive for an automotive fuel pump using a hysteresis comparator," *IEEE Trans. Power Electron.*, vol. 29, no. 3, pp. 1382–1391, Mar. 2014.

[6] K. A. Corzine and S. D. Sudhoff, "A hybrid observer for high performance brushless DC motor drives," *IEEE Trans. Energy Convers.*, vol. 11, no. 2, pp. 318–323, Jun. 1996.

[7] S. Morimoto, M. Sanada, and Y. Takeda, "Sinusoidal current drive system of permanent magnet synchronous motor with low resolution position sensor," in *Proc. IAS Conf. Rec. IEEE Ind. Appl. Conf. 31st IAS Annu. Meeting*, Oct. 1996, pp. 9–14. [Online]. Available: https://ieeexplore.ieee.org/document/556990

[8] J. Bu, L. Xu, T. Sebastian, and B. Liu, "Near-zero speed performance enhancement of PM synchronous machines assisted by low-cost Hall effect sensors," in *Proc. APEC 98 13th Annu. Appl. Power Electron. Conf. Expo.*, Feb. 1998, pp. 64–68. [Online]. Available: https://ieeexplore.ieee.org/document/647670

[9] A. Yoo, S. Sul, D. Lee, and C. Jun, "Novel speed and rotor position estimation strategy using a dual observer for low-resolution position sensors," *IEEE Trans. Power Electron.*, vol. 24, no. 12, pp. 2897–2906, Dec. 2009.

[10] S.-Y. Kim, C. Choi, K. Lee, and W. Lee, "An improved rotor position estimation with vector-tracking observer in PMSM drives with low-resolution Hall-effect sensors," *IEEE Trans. Ind. Electron.*, vol. 58, no. 9, pp. 4078–4086, Sep. 2011.

[11] A. Mousmi, A. Abbou, and Y. El Houm, "Binary diagnosis of Hall effect sensors in brushless DC motor drives," *IEEE Trans. Power Electron.*, vol. 35, no. 4, pp. 3859–3868, Apr. 2020.

[12] Y.-S. Jeong, S.-K. Sul, S. E. Schulz, and N. R. Patel, "Fault detection and fault-tolerant control of interior permanent-magnet motor drive system for electric vehicle," *IEEE Trans. Ind. Appl.*, vol. 41, no. 1, pp. 46–51, Jan. 2005.

[13] R. R. Sorial, M. H. Soliman, H. M. Hasanien, and H. E. A. Talaat, "A vector controlled drive system for electrically power assisted steering using Hall-effect sensors," *IEEE Access*, vol. 9, pp. 116485–116499, 2021.

[14] A. Tashakori and M. Ektesabi, "A simple fault tolerant control system for Hall effect sensors failure of BLDC motor," in *Proc. IEEE 8th Conf. Ind. Electron. Appl. (ICIEA)*, Jun. 2013, pp. 1011–1016. [Online]. Available: https://ieeexplore.ieee.org/doc-ument/6566515

[15] Q. Zhang and M. Feng, "Fast fault diagnosis method for Hall sensors in brushless DC motor drives," *IEEE Trans. Power Electron.*, vol. 34, no. 3, pp. 2585–2596, Mar. 2019.

[16] Y. Zhao, W. Huang, and J. Yang, "Fault diagnosis of low-cost hall-effect sensors used in controlling permanent magnet synchronous motor," in *Proc. 19th Int. Conf. Elect. Mach. Syst. (ICEMS)*, Nov. 2016, pp. 1–5. [Online], Available: https://ieeexplo-re.ieee.org/document/7837472

[17] Q. Ni, M. Yang, S. A. Odhano, M. Tang, P. Zanchetta, X. Liu, and D. Xu, "A new position and speed estimation scheme for position control of PMSM drives using low-resolution position sensors," *IEEE Trans. Ind. Appl.*, vol. 55, no. 4, pp. 3747–3758, Jul. 2019.

[18] L. Dong, J. Jatskevich, Y. Huang, M. Chapariha, and J. Liu, "Fault diagnosis and signal reconstruction of Hall sensors in brushless permanent magnet motor drives," *IEEE Trans. Energy Convers.*, vol. 31, no. 1, pp. 118–131, Mar. 2016.
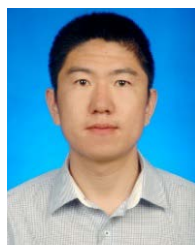
CHUANGQIANG GUO (Member, IEEE) received the Ph.D. degree in mechanical engineering from the Harbin Institute of Technology, China, in 2012. He is currently an Assistant Research Fellow with the State Key Laboratory of Robotics and System, Harbin Institute of Technology. His current research interests include design and control approaches to developing high reliability robotic system that working extreme environment.

XINDONG GAO received the master's degree in mechanical engineering from the Harbin Institute of Technology, China, in 2021. His current research interests include fault detection and fault tolerant control of permanent magnet synchronous motor.

QINGLI ZHANG received the Ph.D. degree in mechanical engineering from the Harbin Institute of Technology, China, in 2011. He is currently a Senior Engineer with the China Academy of Launch Vehicle Technology. His current research interests include design of space motion mechanism, design and application of space robot, and on the technology of landing gear devices.

YINGYUAN ZHU received the Ph.D. degree in mechanical engineering from the Harbin Institute of Technology, China, in 2007. He is currently an Associate Research with the State Key Laboratory of Robotics and System, Harbin Institute of Technology. His current research interest includes the end-effector of robot.

• • •